Bulletin of Electrical Engineering and Informatics
Vol. 13, No. 3, June 2024, pp. 1707~1717
ISSN: 2302-9285, DOI: 10.11591/eei.v13i3.6433

Soil moisture estimation using ground scatterometer and Sentinel-1 data

Geeta T. Desai, Abhay N. Gaikwad
Department of Electronics and Telecommunication Engineering, Babasaheb Naik College of Engineering, Sant Gadge Baba Amravati University, Maharashtra, India

Article Info

Article history:

Received Apr 10, 2023
Revised Sep 11, 2023
Accepted Oct 24, 2023

Keywords:

Generalized regression neural network
Ground scatterometer
Random forest regression
Soil moisture
Support vector regression

ABSTRACT

Soil moisture (SM) is a crucial criterion for agronomics and the management of water resources, particularly in areas where the socio-economic status and significant source of income depend upon agriculture and related sectors. This paper intends to estimate SM over the vegetative area using a generalized regression neural network (GRNN) and ground scatterometer and compare the results with SM retrieved using Sentinel-1 data. At the same time, random forest regression (RFR) and support vector regression (SVR) models are used for SM estimation. Correlation analysis results concluded that L-band HV-polarization at 30^0 incidence angle showed the highest correlation with the measured field parameters. This study investigated backscattering coefficients, VV/VH polarization ratio and polarization phase difference over wheat's entire growth phase to estimate SM. The results indicate that the GRNN with backscattering coefficients and polarization ratio provided the highest accuracy compared to the random forest (RF) and SVR with the root mean square error of 0.093 over the Yavatmal District, Maharashtra, India.

Corresponding Author:

Geeta T. Desai
Department of Electronics and Telecommunication Engineering, Babasaheb Naik College of Engineering
Sant Gadge Baba Amravati University
Maharashtra, India
Email: tgeetadesai@gmail.com

1. INTRODUCTION

Surface soil moisture (SM) is a decisive land criterion for understanding the physical interaction of the land concerning the atmosphere. SM controls our daily lives, environmental factors, agricultural practices, and climatic change. Traditional SM monitoring methods are labour-intensive and need more spatial coverage wherehas satellite remote sensing helps in SM monitoring over a large scale [1], [2]. Agricultural yield is enhanced due to continuous innovations in technology. SM estimation can help in scheduling irrigation which is considered to be a critical issue in agriculture [3]. In the literature, several ways have been suggested for estimating SM, using optical and microwave remote sensing observations. However, optical remote sensing data is masked by clouds as a result of the short wavelength. Microwave remote sensing can get around these shortcomings of optical sensors [4]–[7]. Numerous studies have shown how a ground-based scatterometer (GBS) can be used to monitor SM. Monitoring of soil parameters over vegetation areas for an extensive period increasingly relies on GBS data based on microwave scattering.

For smooth bare soil surfaces, the measured backscatter intensity represents SM. However, for vegetation areas, the SM estimation process becomes complicated due to the complexity of the interaction of microwave signals with soil and vegetation. Hence SM estimation over vegetation soil surfaces is still a

challenging task. Many earlier studies have tried to quantify SM using surface inversion models, vegetation models, and coupling surface inversion models with vegetation models. However, surface inversion models in vegetation areas produce highly uncertain results, which inspired various experiments to make up for the backscatter response for vegetation components. Several methods have been suggested in the literature to estimate SM from full polarimetric scatterometer data. The works in [8], [9] developed an empirical model using multipolarized radar measurements to estimate bare soil's surface SM content. Shi *et al.* [10] developed a single scattering IEM model based on regression analysis for estimating SM from L-band measurements. In [11], using an empirical scattering model, authors retrieved SM from measured backscattering coefficients over vegetative fields. Oh [12] utilized the inversion technique for retrieving surface SM content from multipolarized radar observations. Empirical model was developed for SM extraction over a soybean field using full polarimetric radar data in [13]. In [14], [15], it was observed that using a polarimetric discrimination ratio reduces surface roughness's effect on SM estimation. The co-polarisation ratio's potential for estimating SM was explored using a neuro-fuzzy inference system in [16]. Wang and Mo [17] used co-polarization phase difference (PPD) for corn and orchid fields. Haldar *et al.* [18] used PPD for wheat crops using Sentinel-1 data. In this investigation, we have employed the polarization ratio (PR) and PPD for SM estimation. Previously to the best of our knowledge no researchers have used PPD for GBS data to retrieve SM. GBS installations furnish minute data of a target by modifying incident angle and polarization configuration of the sensor. Hence there is need to research the competance of PPD and PR in SM estimation using GBS data.

Machine learning allows a machine to learn on its own [19]. Machine learning algorithms are capable of setting up a regression relationship between two parameters. Additionally, it serves as a predictive model to forecast the outcome of fresh data [20]. In the proposed, research generalized regression neural network (GRNN), random forest regression (RFR) and support vector regression (SVR) are utilized for soil estimation on full polarimetric GBS data. The study presents an SM retrieval algorithm based on full polarimetric data. The following are the goals of this paper: i) to probe the suitability of PPD and PR for estimating SM; ii) asses the performance of GRNN, RFR and SVR for soil estimation; and iii) compare the results obtained from full polarimetric GBS data with results obtained using Sentinel-1 data. The remaining paper is as follows: section 2 details the study area and wheat plant phenology. Section 3 discusses the methodology, results are discussed in section 4, and section 5 summarizes and concludes the work.

2. STUDY AREA

The farm (19.896536, 77.532668) is located near Pusad city in the Yavatmal District of Maharashtra, India. The site is spread across 7 acres with a smooth topography. Wheat and chickpea are major rabi crops grown in this area. Wheat is sown early in winter and grows from November to May. The duration of wheat crop in India depends upon the type of wheat and environmental conditions. The wheat growth period varies between 110-120 days. The wheat was planted in January 2022 and harvested in April 2022. Figure 1 shows pictures of the wheat crop at different stages during the study. A total of five measurements were taken over the whole wheat growth cycle. The phenological cycle of the wheat crop can be classified as emergence, tillering, stem elongation, boot, flowering, and ripening stages. Figure 1 depicts the state of growth of wheat during field measurements.

Figure 1. Field photographs of wheat in various growth stages

3. METHOD

In this paper, we have presented SM retrieval over the wheat field using a GRNN, RFR and SVR with GBS data and compared the results with SM retrieved using Sentinel-1 data. The flow chart of the presented algorithm for estimating SM is shown in Figure 2. The method consists of five steps: data acquisition, finding optimum incidence angle and polarization, data preparation, SM retrieval and in the last step comparion between results obtained with GBS data and with Sentinel-1 data is done. A detailed explanation of each step is given below.

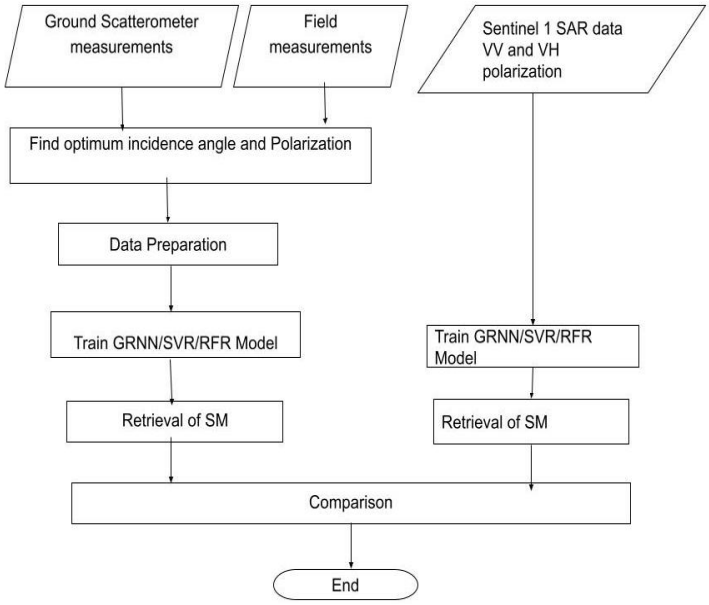

Figure 2. Flowchart for soil estimation using GRNN, SVR, and RFR

3.1. Data acquisition

This section covers the data used in the presented study. The data include GBS data, field measurements of SM and Sentinel-1 data. During the whole growth cycle of wheat crop, backscatter and Sentinel-1 data was acquired from scatterometer and from GEE platform respectively. In situ SM was measured for verification of extracted SM.

3.1.1. Ground scatterometer measurement

The multifrequency polarimetric GBS utilized in this investigation comprises of L and S-band horn antennas having a gain of 20 db, a vector network analyzer (VNA, 1-4 GHz), radio-frequency cables and a personal computer for data storage. The polarimetric scatterometer operates in a stepped frequency sweep mode with all horizontal (H) and vertical (V) polarization combinations. The scatterometer is mounted on a wooden platform to measure the backscattering coefficient, including two bands (L and S), full-polarizations (VV, VH, HV, HH), and incidence angles from 0° to 70° in steps of 5°. From January to April 2022, experimental data, including backscatter and ground data, were collected five times in synchronization with satellite revisit time on the wheat field near Pusad, Maharashtra.

3.1.2. Field measurements

SM was measured using the direct method. Five random points were selected from the investigation site during each data acquisition to collect soil samples. Soil specimens were gathered from a distance of 10 cm from the soil surface, and they were packed in air-tight polythene bags. The collected samples were oven-dried in the laboratory. The SM was calculated by calculating the weight difference of the soil samples before and after drying. The average value of five measurements was taken to calculate SM. The average plant height, leaf length and stem width were calculated by measuring plant height, leaf length and stem width at five different locations in the wheat crop bed. Figure 3 shows the temporal variation of crop growth variables such as plant height, leaf length, and stem width of the wheat crop. All the crop growth variables of the wheat crop were found to increase with the crop growth.

3.1.3. Sentinel-1 data

We have used the data set consisting of Sentinel-1 data and field measurements of soil and vegetation growth parameters collected over wheat crop in the Haouz plain in Morocco dataset [21] for training GRNN/SVR and RFR algorithm. VH and VV backscattering coefficients at the study location on data acquisition dates were acquired using Google Earth Engine to validate retrieved SM using Sentinel-1 data. Sentinel-1 is a synthetic aperture radar operating in interferometric wide (IW) swath mode at a frequency of 5.33 GHz in the C band. The primary operational imaging mode is the (IW) swath mode covering incidence angles between 31º and 46º.

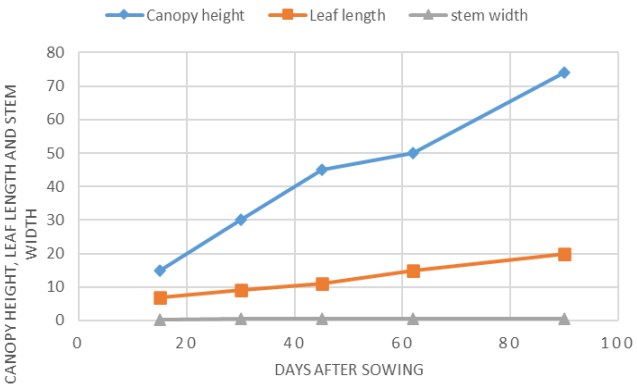

Figure 3. Temporal variation of crop growth variables of wheat crop

3.2. Finding optimum system configuration

Correlation analysis was conducted to determine the ideal incidence angle and polarization of GBS for estimating SM. The correlation coefficient's value fluctuates between +1 and -1 depending on how strong the association is between two variables. After applying correlation analysis between ground parameters and backscattering value for different polarizations, HV polarization with 30^0 incidence angle is found optimal for operation.

3.3. Data preparation

To estimate SM PR and PPD with backscattering coefficients are utilized in the algorithm. For data preparation the PR and PPD were computed using (1) and (2). The data (backscattering coefficient, PR and PPD) of the wheat crop at a 30° angle of incidence for the L band at HV polarization was interpolated in 91 data sets which were further divided into 63 and 28 data sets for training and testing respectively. The detailed explanation about polarization ratio and polarization phase difference is given in following sections.

3.3.1. Polarization ratio

The polarization ratio is the ratio of VH and VV polarized scattering coefficients. It is calculated by (1) [22]. PR is more persistent than the backscattering coefficient for both polarizations, VV and VH. Previous studies [18] have confirmed that PR reduces the effect of soil roughness and gives a more accurate estimation of SM.

$$PR = \frac{\sigma_{VH}}{\sigma_{VV}} \quad (1)$$

3.3.2. Polarization phase difference

The co-polarization phase difference was calculated using (2) [23]:

$$\emptyset_c = \emptyset_{HH} - \emptyset_{VV} \quad (2)$$

where $\emptyset c$ is the relative phase difference and is equal to the absolute phase difference between co-polarized HH and VV polarization, the HH and VV phase difference consists of vital information at par with cross-polarized phase difference in two polarization channels [18]. The investigation focuses on relating the changes in phase difference to SM.

3.4. Soil moisture retrieval

We implemented three regression models GRNN, SVR, and RFR based on machine learning for the direct estimation of SM. To investigate the suitability of backscattering coefficients and various polarimetric data-derived vegetation descriptors for estimating the SM of wheat GRNN, SVR, and RFR models were tested for different combinations of polarization ratio and polarization phase difference with backscattering coefficient.

3.4.1. Generalized regression neural network

GRNN was first developed by Specht, similar to radial basis function networks [24]. GRNN has applications in different fields like time series prediction, adaptive control and pattern recognition. The key benefit of this type of neural network is that iterative training is not required. Instead, direct computation of functional estimates can be obtained from the training data. The architecture of GRNN is shown in Figure 4. GRNN comprises four layers (the input layer, the pattern layer, the summation layer, and the output layer). Each neuron in the pattern layer represents a training pattern and admits input from the input layer. The output from each neuron measures how much the input deviates from the stored pattern.

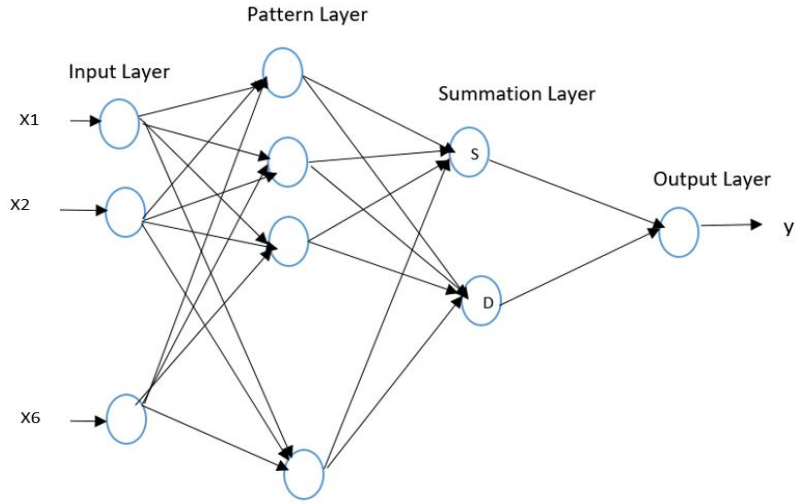

Figure 4. GRNN architecture

In the summation layer, one type of neuron calculates the sum of the weighted output of pattern neurons and the other type computes the unweighted results of the pattern layer. Finally, normalization is performed by the output layer to calculate value of the output variable predicted by GRNN. In the proposed work, the input vector x of the GRNNs used to retrieve SM includes backscattering coefficients, PPD and PR for GBS and backscattering coefficients and PR of the Sentinel-1 dataset.

3.4.2. Support vector regression model

SVR is based on a support vector machine (SVM) and was first invented by Vapnik. SVM handles both classification and regression tasks. The SVR performs the estimation task by input-output dataset mapping. It focuses on class boundaries and applies a non-linear transformation to map the input space created by independent variables using the kernel function [25]. Linear, polynomial and radial basis function are different kernels available in SVM. The radial basis function kernel is the most frequently used in several previous studies [26]. In high dimensional space, an ideal linear separator is found that optimizes the margin between the classes [27], [28]. The generalized solution is obtained by maximizing the margin and reducing overfitting. SVR is chosen in presented research since it is best suited for small input sampling sizes, has limited complexity and high stability of the learning process.

3.4.3. Random forest regression model

Random forest (RF) is a machine learning model that efficiently performs classification and regression functions. RF is developed by the bagging technique [29]. The RFR model operates by forming regression trees and choosing the finest split at each node by applying predictor variables [29], [30]. Each tree is created by repetitively separating the population based on optimising a split rule over the

p-dimensional covariate space. At every split, each node is divided into two daughter nodes. Until the terminal node is achieved, daughter nodes are split, and the terminal node is defined by stopping criteria dependent on node purity or node member size. In regression tasks, mean square error is used, whereas for classification applications Gini index is used for split rule. The final RF result for the regression task is obtained by aggregating, averaging (regression) or voting (classification) of each terminal node [31].

3.5. Comparison

In this step the outcomes of the two suggested methods one based on the GBS data and others on Sentinel-1 data, are compared. The metrics for comparison include the root mean squared error (RMSE). RMSE is used to assess the performance of the developed algorithm for SM estimation. RMSE is defined as (3):

$$\text{RMSE} = \sqrt{\frac{1}{N}\sum_{i=1}^{N}(SM_m - SM_o)^2} \quad (3)$$

Where SM_m is the estimated SM, SM_o is the observed or original SM, and N stands for number of observations.

4. RESULTS AND DISCUSSION

4.1. Variation of backscattering coefficients with polarization

Figure 5 shows temporal variation of backscattering coefficients at optimum incidence angle. It can be observed that polarized backscattering coefficients are higher than the cross-polarized backscattering coefficient. The range of the backscattering coefficient is from -60 to -40 db for L and S band. As wheat grew, an initial rise in backscattering coefficients was observed till the heading stage which reduced until the harvesting stage. The backscatter coefficients slightly increase with a decrease in frequency. During the study, S-band showed lower backscatter coefficients than the L-band.

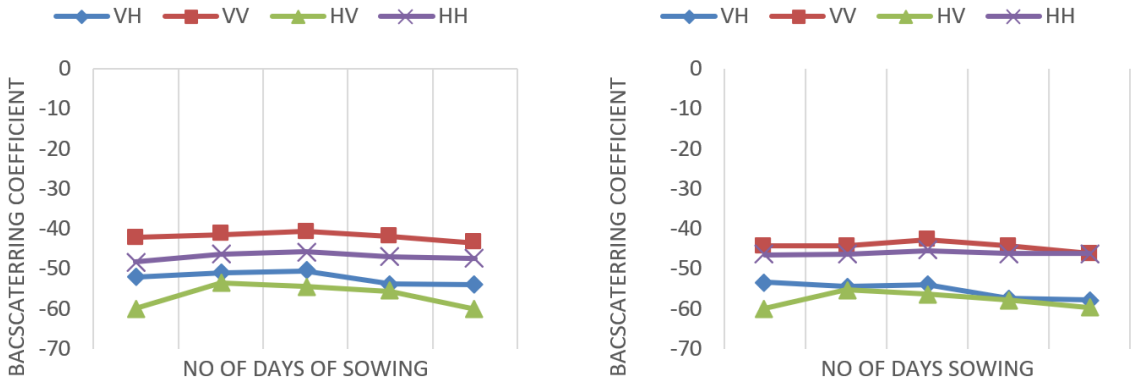

Figure 5. Temporal variation of backscaterring at 30º incidence angles at L and S band

4.2. Optimum parameter selection of GBS

For selecting the optimum parameters of the GBS, correlation analysis was conducted between crop variables and the backscattering coefficient to determine the most suitable incidence angle for the operation of the scatterometer. Correlation analysis was done between σº and vegetation growth parameters to find the correlation coefficient between them and determine the optimum parameters of the GBS, as summarized in Tables 1 and 2 for Lband and Tables 3 and 4 for S band. After applying correlation analysis between ground parameters and backscattering value for different polarization, HV polarization with 30º incidence angle is optimal for operation.

4.3. Estimation of soil moisture

This section focuses on retrieving the SM throughout the growing season of the wheat crop. The SM is estimated using both scatterometer and Sentinel-1 data using GRNN, SVR and RFR model. The outcomes of the two suggested methods one based on the GBS data and others on Sentinel-1 data, are compared and discussed in this section.

Table 1. Correlation coefficients between backscatter coefficients and ground parameters at Lband for VV and VH polarization

Incidence angle	Correlation coefficient **VV**				Correlation coefficient **VH**			
	CH	LL	SW	SM	CH	LL	SW	SM
10	0.14	0.35	-0.12	0.03	-0.53	-0.46	-0.8	0.68
15	-0.4	-0.17	-0.65	0.51	-0.59	-0.52	-0.82	0.74
20	-0.39	-0.16	-0.65	0.5	-0.67	-0.59	-0.82	0.82
25	-0.32	-0.09	-0.59	0.44	-0.69	-0.61	-0.84	0.83
30	-0.14	0.1	-0.42	0.27	-0.69	-0.61	-0.86	0.83
35	-0.14	0.09	-0.43	0.27	-0.66	-0.57	-0.83	0.82
40	-0.06	0.17	-0.33	0.18	-0.72	-0.66	-0.89	0.83
45	0	0.23	-0.25	0.11	-0.71	-0.64	-0.86	0.84
50	0	0.23	-0.25	0.11	-0.72	-0.64	-0.84	0.86
55	0	0.23	-0.24	0.11	-0.6	-0.61	-0.37	0.39
60	-0.01	0.22	-0.27	0.13	-0.62	-0.53	-0.85	0.77
65	-0.01	0.22	-0.27	0.13	-0.59	-0.51	-0.85	0.75
70	0	0.24	-0.27	0.12	-0.2	-0.06	-0.65	0.4

Table 2. Correlation coefficients between backscatter coefficients and ground parameters at Lband for HH and HV polarization

Incidence angle	Correlation coefficient **HH**				Correlation coefficient **HV**			
	CH	LL	SW	SM	CH	LL	SW	SM
10	0.19	-0.03	0.63	-0.31	-0.68	-0.78	-0.18	0.61
15	0.22	0.01	0.68	-0.37	-0.68	-0.78	-0.16	0.55
20	0.08	-0.13	0.39	-0.11	-0.67	-0.76	-0.14	0.54
25	0.22	0.01	0.68	-0.37	-0.67	-0.77	-0.15	0.54
30	0.14	-0.07	0.62	-0.3	**-0.78**	**-0.68**	**-0.96**	**0.89**
35	0.2	-0.01	0.67	-0.35	-0.66	-0.76	-0.13	0.51
40	0.08	-0.12	0.58	-0.23	-0.66	-0.77	-0.14	0.53
45	-0.08	-0.29	0.43	-0.06	-0.6	-0.73	-0.07	0.46
50	-0.08	-0.29	0.43	-0.07	-0.51	-0.66	0.03	0.39
55	-0.23	-0.42	0.31	0.08	-0.46	-0.62	0.09	0.34
60	-0.11	-0.32	0.4	-0.05	-0.38	-0.52	0.19	0.27
65	-0.15	-0.35	0.37	-0.02	-0.55	-0.67	-0.01	0.46
70	-0.19	-0.4	0.31	0.02	-0.64	-0.77	-0.12	0.51

Table 3. Correlation coefficients between backscatter coefficients and ground parameters at S band for VV and VH band

Incidence angle	Correlation coefficient **VV**				Correlation coefficient **VH**			
	CH	LL	SW	SM	CH	LL	SW	SM
10	0.2	0.35	-0.12	0.03	-0.78	-0.63	-0.93	0.78
15	-0.4	-0.17	-0.65	0.51	-0.77	-0.63	-0.93	0.77
20	-0.39	-0.16	-0.65	0.5	-0.75	-0.61	-0.94	0.75
25	-0.32	-0.09	-0.59	0.44	-0.76	-0.62	-0.94	0.76
30	-0.14	0.1	-0.42	0.27	-0.78	-0.64	-0.93	0.79
35	-0.14	0.09	-0.43	0.27	-0.78	-0.63	-0.94	0.78
40	-0.06	0.17	-0.33	0.18	-0.71	-0.55	-0.91	0.73
45	0	0.23	-0.25	0.11	-0.72	-0.57	-0.91	0.74
50	0	0.23	-0.25	0.11	-0.76	-0.62	-0.94	0.76
55	0	0.23	-0.24	0.11	-0.6	-0.57	-0.49	0.42
60	-0.01	0.22	-0.27	0.13	-0.7	-0.52	-0.87	0.72
65	-0.01	0.22	-0.27	0.13	-0.72	-0.55	-0.91	0.74
70	0	0.24	-0.27	0.12	-0.76	-0.61	-0.93	0.77
75	0	0.23	-0.28	0.13	-0.78	-0.64	-0.94	0.79

4.3.1. Using scatterometer data

The proposed algorithm was tested on four different input configurations that is: i) backscattering coefficient, ii) backscattering coefficient+PR, iii) backscaterring coefficients+PPD, and iv) backscattering coefficient+PR+PPD to analyse the impact of various polarimetric features. Figures 6(a) to (c) shows the relationship between measured SM and those predicted using GRNN, RFR and SVR respectively with five-fold cross-validation. In Table 5, obtained RMSE and MSE for different combinations of GBS data using GRNN, SVR, and RF is tabulated. With RMSE between 0.177 and 0.093, GRNN based estimation achieved the best accuracy. For SVR, the RMSE values ranged between 0.931 and 0.785, for RF regression obtained,

RMSE varies between 0.269 and 0.130. In all three cases, results indicate that the combination of backscattering data, PR and PPD exhibits the best performance compared to the other two combinations. For SM estimation all models were found suitable, but the performance of GRNN was best as compared to RFR and SVR. Furthermore, the obtained results were better than [16] due to the addition of full polarimetric data-derived vegetation descriptors PPD and PR for estimating SM.

Table 4. Correlation coefficients between backscatter coefficients and ground parameters at S band for HH and HV polarization

Incidence angle	Correlation coefficient **HH**				Correlation coefficient **HV**			
	CH	LL	SW	SM	CH	LL	SW	SM
10	0.7	0.57	0.98	-0.78	0.06	-0.15	0.34	-0.07
15	0.66	0.65	0.76	-0.77	-0.78	-0.87	-0.32	0.64
20	0.06	-0.14	0.35	-0.08	-0.79	-0.88	-0.34	0.65
25	0.63	0.67	0.68	-0.71	-0.79	-0.88	-0.34	0.65
30	0.62	0.68	0.66	-0.68	**-0.75**	**-0.65**	**-0.96**	**0.86**
35	0.54	0.55	0.65	-0.68	-0.79	-0.89	-0.36	0.65
40	0.49	0.43	0.53	-0.68	-0.78	-0.87	-0.31	0.65
45	0.69	0.68	0.75	-0.81	-0.79	-0.89	-0.34	0.67
50	0.75	0.78	0.71	-0.83	-0.8	-0.9	-0.35	0.67
55	-0.46	-0.33	-0.68	0.38	-0.78	-0.88	-0.32	0.65
60	-0.88	-0.83	-0.74	0.77	-0.77	-0.86	-0.3	0.62
65	-0.37	-0.41	0.15	0.23	-0.82	-0.9	-0.38	0.71
70	0.76	0.78	0.85	-0.76	-0.78	-0.88	-0.32	0.66
75	-0.81	-0.75	-0.61	0.69	-0.61	-0.74	-0.08	0.47

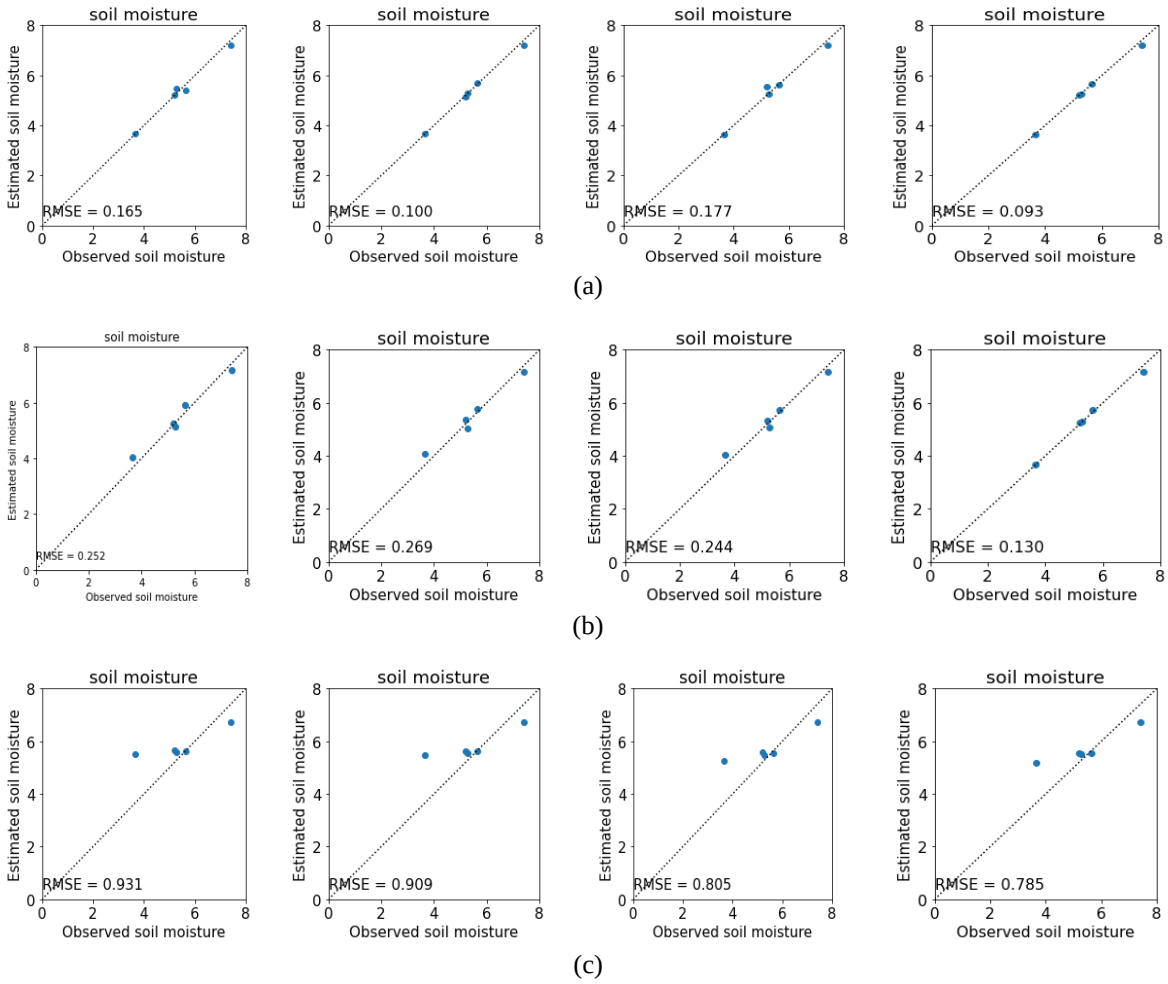

Figure 6. Retrieved SM versus in situ soil measurements for; (a) GRNN, (b) RFR, and (c) SVR using GBS data

Table 5. RMSE and MSE for SM using GRNN, SVR, and RF regressor for GBS data

Data	GRNN		SVR		RFR	
	RMSE	MSE	RMSE	MSE	RMSE	MSE
Backscaterring coefficient	0.165	0.027	0.931	0.866	0.252	0.0637
Backscattering coefficient+PR	0.100	0.0099	0.909	0.82	0.269	0.072
Backscaterring coefficients+PPD	0.177	0.031	0.805	0.64	0.244	0.059
Backscattering coefficient+PR+PPD	0.093	0.0087	0.785	0.61	0.130	0.016

4.3.2. Using Sentinel-1 data

Sentinel-1 datasets and in situ measurements of soil collected over the wheat crop in the Haouz plain in Morocco dataset [19] are used for training the GRNN/SVM and RFR algorithm. VH and VV backscattering coefficients at the study location on data acquisition dates are acquired using Google Earth Engine. These backscattering coefficients are used for validation. Estimated SM is validated with field measurements. The proposed algorithm was tested for two input configurations to analyze the impact of various polarimetric features using GRNN, RFR, and SVR. In Table 6, obtained RMSE, MSE for GBS data with vegetation descriptors PR are mentioned. The results conclude that GRNN gives the best accuracy with an RMSE of 0.962 with a backscattering coefficient and polarization ratio. Figure 7 depicts comparison between SM estimated using GBS and Sentinel-1 data. A correlation of 0.84 is obtained between SM estimated using GBS and Sentinel-1 data.

Table 6. RMSE and MSE for SM using GRNN, SVR and RF regressor for Sentinel-1 data

Data	GRNN		SVM		RF	
	RMSE	MSE	RMSE	MSE	RMSE	MSE
Backscaterring coefficient	1.045	1.091	1.063	1.129	1.082	1.17
Backscattering coefficient +PR	0.962	0.9262	1.057	1.11	1.018	1.03

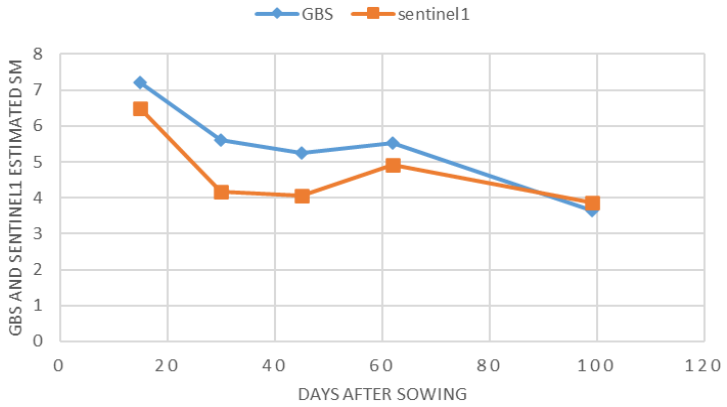

Figure 7. Comparison between SM estimated using Sentinel-1 and GBS data

5. CONCLUSION

The polarimetric radar backscatters of a wheat field were measured using the ground-based L and S-band polarimetric scatterometer in an angular range from 10º to 70º. The suitable incidence angle for the estimation of SM for vegetation was found to be 30º for HV polarization. First, the PPD and PR were analyzed, and then the SM of the wheat field was retrieved using machine learning algorithms. All models were found suitable, but the performance of GRNN was better compared to RFR and SVR's estimation of SM. Finally, the retrieved SM content was compared with the in-situ measured SM content. In future full polarimetric data derived vegetation descriptors, PPD and PR can be used for monitoring conditions of crops and yield predictions.

REFERENCES

[1] E. Tronquo, H. Lievens, J. Bouchat, P. Defourny, N. Baghdadi, and N. E. C. Verhoest, "Soil moisture retrieval using multistatic L-Band SAR and effective roughness modeling," *Remote Sensing*, vol. 14, no. 7, Mar. 2022, doi: 10.3390/rs14071650.

[2] M. G. Kibria and M. T. A. Seman, "Internet of things based automated agriculture system for irrigating soil," *Bulletin of Electrical Engineering and Informatics*, vol. 11, no. 3, pp. 1752–1764, Jun. 2022, doi: 10.11591/eei.v11i3.3554.

[3] L. Rabhi, N. Falih, L. Afraites, and B. Bouikhalene, "Digital agriculture based on big data analytics: a focus on predictive irrigation for smart farming in Morocco," *Indonesian Journal of Electrical Engineering and Computer Science*, vol. 24, no. 1, pp. 581-589, Oct. 2021, doi: 10.11591/ijeecs.v24.i1.pp581-589.
[4] Y. Li, S. Yan, N. Chen, and J. Gong, "Performance evaluation of a neural network model and two empirical models for estimating soil moisture based on Sentinel-1 sar data," *Progress In Electromagnetics Research C*, vol. 105, pp. 85–99, 2020, doi: 10.2528/PIERC20071601.
[5] N. Bhogapurapu, D. Mandal, Y. S. Rao, and A. Bhattacharya, "Soil moisture retrieval using SAR derived vegetation descriptors in water cloud model," in *IGARSS 2020-2020 IEEE International Geoscience and Remote Sensing Symposium*, Sep. 2020, pp. 4696–4699, doi: 10.1109/IGARSS39084.2020.9323699.
[6] D. Singh, R. Prakash, N. P. Pathak, S. Mohan, and K. P. Singh, "SAR and optical data utilization for soil moisture retrieval in vegetated region," in *2011 3rd International Asia-Pacific Conference on Synthetic Aperture Radar, APSAR 2011*, 2011, pp. 790–793.
[7] G. T. Desai and A. N. Gaikwad, "Automatic land cover classification with SAR imagery and machine learning using Google Earth Engine," *International journal of electrical and computer engineering systems*, vol. 13, no. 10, pp. 909–916, Dec. 2022, doi: 10.32985/ijeces.13.10.6.
[8] Y. Oh, K. Sarabandi, and F. T. Ulaby, "An empirical model and an inversion technique for radar scattering from bare soil surfaces," *IEEE Transactions on Geoscience and Remote Sensing*, vol. 30, no. 2, pp. 370–381, Mar. 1992, doi: 10.1109/36.134086.
[9] K. S. Rao, S. Raju, and J. R. Wang, "Estimation of soil moisture and surface roughness parameters from backscattering coefficient," *IEEE Transactions on Geoscience and Remote Sensing*, vol. 31, no. 5, pp. 1094–1099, 1993, doi: 10.1109/36.263781.
[10] Jiancheng Shi, J. Wang, A. Y. Hsu, P. E. O'Neill, and E. T. Engman, "Estimation of bare surface soil moisture and surface roughness parameter using L-band SAR image data," *IEEE Transactions on Geoscience and Remote Sensing*, vol. 35, no. 5, pp. 1254–1266, 1997, doi: 10.1109/36.628792.
[11] S.-G. Kwon, J.-H. Hwang, and Y. Oh, "Estimation of soil moisture from X-band backscattering coefficients of vegetation fields," in *IEICE Proceedings Series*, 2011.
[12] Y. Oh, "Quantitative retrieval of soil moisture content and surface roughness from multipolarized radar observations of bare soil surfaces," *IEEE Transactions on Geoscience and Remote Sensing*, vol. 42, no. 3, pp. 596–601, Mar. 2004, doi: 10.1109/TGRS.2003.821065.
[13] S.-G. Kwon, J.-H. Hwang, and Y. Oh, "Soil moisture inversion from X-band SAR and scatterometer data of vegetation fields," in *2011 IEEE International Geoscience and Remote Sensing Symposium*, Jul. 2011, pp. 3140–3143, doi: 10.1109/IGARSS.2011.6049884.
[14] D. Singh and V. Dubey, "Microwave bistatic polarization measurements for retrieval of soil moisture using an incidence angle approach," *Journal of Geophysics and Engineering*, vol. 4, no. 1, pp. 75–82, Mar. 2007, doi: 10.1088/1742-2132/4/1/009.
[15] D. Singh, "Polarization discrimination ratio approach to retrieve bare soil moisture at X-band," in *Proceedings. 2005 IEEE International Geoscience and Remote Sensing Symposium, 2005. IGARSS '05.*, 2005, vol. 1, pp. 408–411, doi: 10.1109/IGARSS.2005.1526195.
[16] A. K. Vishwakarma and R. Prasad, "Bistatic scatterometer measurements for soil moisture estimation using grid partition-based neuro-fuzzy inference system at l-band," in *Sustainable Development Practices Using Geoinformatics*, Wiley, 2020, pp. 47–56.
[17] J. R. Wang and T. Mo, "The polarization phase difference of orchard trees," *International Journal of Remote Sensing*, vol. 11, no. 7, pp. 1255–1265, Jul. 1990, doi: 10.1080/01431169008955091.
[18] D. Haldar, P. Rana, M. Yadav, R. S. Hooda, and M. Chakraborty, "Time series analysis of co-polarization phase difference (PPD) for winter field crops using polarimetric C-band SAR data," *International Journal of Remote Sensing*, vol. 37, no. 16, pp. 3753–3770, Aug. 2016, doi: 10.1080/01431161.2016.1204024.
[19] S. Tangwannawit and P. Tangwannawit, "An optimization clustering and classification based on artificial intelligence approach for internet of things in agriculture," *IAES International Journal of Artificial Intelligence (IJ-AI)*, vol. 11, no. 1, pp. 201–209, Mar. 2022, doi: 10.11591/ijai.v11.i1.pp201-209.
[20] M. H. X. Wai, A. Huong, and X. Ngu, "Soil moisture level prediction using optical technique and artificial neural network," *International Journal of Electrical and Computer Engineering (IJECE)*, vol. 11, no. 2, pp. 1752–1760, Apr. 2021, doi: 10.11591/ijece.v11i2.pp1752-1760.
[21] N. Ouaadi *et al.*, "C-band radar data and in situ measurements for the monitoring of wheat crops in a semi-arid area (center of Morocco)," *Earth System Science Data*, vol. 13, no. 7, pp. 3707–3731, Jul. 2021, doi: 10.5194/essd-13-3707-2021.
[22] F. Greifeneder *et al.*, "The added value of the VH/VV polarization-ratio for global soil moisture estimations from scatterometer data," *IEEE Journal of Selected Topics in Applied Earth Observations and Remote Sensing*, vol. 11, no. 10, pp. 3668–3679, Oct. 2018, doi: 10.1109/JSTARS.2018.2865185.
[23] F. T. Ulaby, D. Held, M. C. Donson, K. C. McDonald, and T. B. A. Senior, "Relating polaization phase difference of SAR signals to scene properties," *IEEE Transactions on Geoscience and Remote Sensing*, vol. GE-25, no. 1, pp. 83–92, Jan. 1987, doi: 10.1109/TGRS.1987.289784.
[24] D. F. Specht, "A general regression neural network," *IEEE Transactions on Neural Networks*, vol. 2, no. 6, pp. 568–576, 1991, doi: 10.1109/72.97934.
[25] V. Vapnik, "The support vector method of function estimation," in *Nonlinear Modeling*, Boston, MA: Springer US, 1998, pp. 55–85.
[26] D. Gupta, P. Rajendra, M. Narayan, V. Ajeet, and S. Kumar, "Support vector regression for retrieval of soil moisture using bistatic scatterometer data at X-band," *International Journal of Geological and Environmental Engineering*, vol. 9, no. 10, pp. 1201–1204, 2015.
[27] A. J. Smola and B. Schölkopf, "A tutorial on support vector regression," *Statistics and Computing*, vol. 14, no. 3, pp. 199–222, Aug. 2004, doi: 10.1023/B:STCO.0000035301.49549.88.
[28] L. Pasolli, C. Notarnicola, and L. Bruzzone, "Estimating soil moisture with the support vector regression technique," *IEEE Geoscience and Remote Sensing Letters*, vol. 8, no. 6, pp. 1080–1084, Nov. 2011, doi: 10.1109/LGRS.2011.2156759.
[29] L. Andy and W. Matthew, "Classification and regression by randomforest," *R News*, vol. 2, pp. 18–22, 2002.
[30] W. Loh, "Classification and regression trees," *WIREs Data Mining and Knowledge Discovery*, vol. 1, no. 1, pp. 14–23, Jan. 2011, doi: 10.1002/widm.8.
[31] J. Ehrlinger, "ggRandomForests: Visually exploring a random forest for regression," *arXiv*, Jan. 2015, doi: 10.48550/arXiv.1501.07196.

BIOGRAPHIES OF AUTHORS

Geeta T. Desai received her BE degree from Padre Conceicao College of Engineering, Verna, Goa University, ME in Electronics and Telecommnication Engineering from the Mumbai University in 2014, and she is pursuing Ph.D. degree in Electronics from Babasaheb Naik College of Engineering, Pusad from Amravati University. She is working as an Assistant Professor in Electronics and Department of Computer, in Anjuman-I-Islam's Kalsekar Technical Campus. Her current research interests include digital image processing, remote sensing, and machine learning. She can be contacted at email: tgeetadesai@gmail.com.

Abhay N. Gaikwad received his BE degree from Babasaheb Naik College of Engineering, Pusad, Amravati University, Amravati in 1993, M.Tech from VNIT(formerly VRCE) Nagpur in 2001 and Ph.D. from Indian Institute of Technology, Roorkee, Uttarakhand, India in 2012. He is presently working as Professor in Department of Electronics and Telecommunication Engineering, Babasaheb Naik College of Engineering Pusad. He has 26 years of experience in teaching. His research interest includes wireless communication, radar signal processing, and through wall imaging radar. He can be contacted at email: abhay.n.gaikwad@gmail.com.